Biol Blood Marrow Transplant 24 (2018) 666–677

Biology of Blood and Marrow Transplantation

journal homepage: www.bbmt.org

ASBMT American Society for Blood and Marrow Transplantation

Biology

Increased Coexpression of PD-1, TIGIT, and KLRG-1 on Tumor-Reactive CD8⁺ T Cells During Relapse after Allogeneic Stem Cell Transplantation

Tim J.A. Hutten [1], Wieger J. Norde [1], Rob Woestenenk [1], Ruo Chen Wang [1], Frans Maas [1], Michel Kester [2], J.H. Frederik Falkenburg [2], Sofia Berglund [3], Leo Luznik [3], Joop H. Jansen [1], Nicolaas Schaap [4], Harry Dolstra [1,†], Willemijn Hobo [1,†,*]

[1] *Department of Laboratory Medicine—Laboratory of Hematology, Radboud University Medical Center, Nijmegen, The Netherlands*
[2] *Department of Hematology, Leiden University Medical Center, Leiden, The Netherlands*
[3] *Department of Oncology and Hematologic Malignancies, The Johns Hopkins University School of Medicine, Baltimore, Maryland*
[4] *Department of Hematology, Radboud University Medical Center, Nijmegen, The Netherlands*

Article history:
Received 18 August 2017
Accepted 22 November 2017

Key Words:
MiHA
Allo-SCT
PD-1
TIGIT and T cells

A B S T R A C T

Allogeneic stem cell transplantation (allo-SCT) can be a curative treatment for patients with a hematologic malignancy due to alloreactive T cell responses recognizing minor histocompatibility antigens (MiHA). Yet tumor immune escape mechanisms can cause failure of T cell immunity, leading to relapse. Tumor cells display low expression of costimulatory molecules and can up-regulate coinhibitory molecules that inhibit T cell functionality on ligation with their counter-receptors on the tumor-reactive T cells. The aim of this explorative study was to evaluate immune checkpoint expression profiles on T cell subsets and on cytomegalovirus (CMV)- and/or MiHA-reactive CD8⁺ T cells of allo-SCT recipients using a 13-color flow cytometry panel, and to correlate these expression patterns to clinical outcomes. MiHA-reactive CD8⁺ T cells exhibited an early differentiated CD27⁺⁺/CD28⁺⁺ phenotype with low KLRG-1 and CD57 expression. These T cells also displayed increased expression of PD-1, TIM-3, and TIGIT compared with total effector memory T cells and CMV-specific CD8⁺ T cells in healthy donors and allo-SCT recipients. Remarkably, high coexpression of PD-1, TIGIT, and KLRG-1 on MiHA-reactive CD8⁺ T cells was associated with relapse after allo-SCT. Taken together, these findings indicate that MiHA-specific CD8⁺ T cells of relapsed patients have a distinctive coinhibitory expression signature compared with patients who stay in remission. This phenotype may serve as a potential monitoring tool in patients. Moreover, these findings suggest that PD-1 and TIGIT play important roles in regulating T cell-mediated tumor control, providing a rationale for immunotherapy with blocking antibodies to treat relapse after allo-SCT.

INTRODUCTION

Immunotherapy is a potent treatment modality in hematologic malignancies. A well-established example in this regard is allogeneic stem cell transplantation (allo-SCT) [1,2], in which a patient receives a donor hematopoietic stem cell graft to replace host hematopoiesis and to invoke a graft-versus-tumor (GVT) immune response toward residual malignant cells. One important aspect in establishing successful GVT immunity is the induction of donor CD8⁺ T cell responses targeting recipient-specific minor histocompatibility antigens (MiHAs) and tumor-associated antigens expressed by residual tumor cells. Upon activation, these T cells acquire effector functions, and thereby the capacity to eradicate the malignant cells [3,4].

Although allo-SCT can be curative due to establishment of long-lived tumor-reactive T cell memory, relapse remains the leading cause of treatment failure [5,6]. Tumor cells evade T cell immunity by exploiting different mechanisms. Low expression of costimulatory molecules in combination with increased expression of coinhibitory molecules by the tumor cells is associated with poor prognosis [7]. Tumor-reactive T cells can up-regulate coinhibitory receptors, including CTLA-4, PD-1, and TIM-3, and subsequent inhibitory signaling dampens T cell functionality [8-11]. We and others have

Financial disclosure: See Acknowledgments on page 676.

* Correspondence and reprint requests: Willemijn Hobo, PhD, Department of Laboratory Medicine-Laboratory of Hematology, Radboud University Medical Center, Geert Grooteplein 8, PO Box 9101, 6500 HB Nijmegen, The Netherlands.
E-mail address: Willemijn.Hobo@Radboudumc.nl (W. Hobo).
† Authors contributed equally.

https://doi.org/10.1016/j.bbmt.2017.11.027

previously demonstrated the inhibitory role of PD-1 and BTLA on tumor-reactive T cell functionality in transplant recipients [12-14]. In recent years, antagonistic antibodies against PD-1 and CTLA-4 have been investigated for treatment of multiple cancers, with impressive improvements in disease outcomes [15-17]. However, not all patients respond, and others acquire resistance to these checkpoint blockers. Recently, a plethora of new coinhibitory molecules have been implicated in tumor immune escape [8,18-22]. It has been demonstrated that signaling through multiple coinhibitory molecules on the same T cell can aggravate T cell dysfunction [8,23]. In this context, it has been shown that simultaneous blockade of 2 or even 3 coinhibitory molecules, such as PD-1 and CTLA-4, leads to synergistic improvement of antitumor T cell responses [20,24]. This prompted us to investigate the expression profiles of a comprehensive panel of cosignaling receptors on MiHA-specific $CD8^+$ T cells of patients after allo-SCT and to analyze these in relation to clinical outcome.

Here we analyzed the expression of 15 cosignaling molecules on T cell subsets of allo-SCT recipients (n = 30) and healthy donors (n = 10) by 13-color flow cytometry. Using tetramer technology, we identified (low-frequency) circulating antigen-specific $CD8^+$ T cells (cytomegalovirus [CMV], MiHA). We observed distinct coexpression profiles of cosignaling molecules during T cell differentiation. Importantly, MiHA-specific $CD8^+$ T cells retained an early differentiated phenotype with high expression of the costimulatory molecules CD27 and CD28, whereas CD57 expression was relatively low. In addition, these T cells showed increased levels of PD-1, TIM-3, and TIGIT. Of note, high coexpression of PD-1, TIGIT, and KLRG-1 on MiHA-specific $CD8^+$ T cells was associated with relapse after allo-SCT. Taken together, the data from our explorative study suggest that multiple cosignaling molecules may act together in regulating T cell-mediated tumor control. Treatment with antibodies targeting multiple cosignaling molecules would be an attractive adjuvant treatment strategy to boost the potency of these highly activated, potentially dysfunctional, tumor-reactive T cells for treatment of relapse after allo-SCT.

MATERIALS AND METHODS

Patient and Donor Material

Peripheral blood mononuclear cells (PBMCs) were isolated using Ficoll-Hypaque (GE Life Sciences Healthcare, Chicago, IL) density centrifugation of healthy donor buffy coats (Sanquin, Nijmegen, The Netherlands) or peripheral blood of allo-SCT recipients. Healthy donors were selected for HLA-B7 positivity and presence of CMV-specific $CD8^+$ T cells. Allo-SCT recipient-donor pairs were screened for MiHA disparity using allele-specific PCR [25]. Patients were selected based on detectable MiHA- or CMV-specific $CD8^+$ T cell responses following allo-SCT [4]. Patients were treated as described previously [4]; characteristics are summarized in Table 1 and Tables S1 and S2. Patient and donor material and data were obtained in accordance with the Declaration of Helsinki and institutional guidelines and regulations (CMO 2013/064).

Flow Cytometry

Expression of coinhibitory and costimulatory molecules on PBMCs of healthy donors and allo-SCT recipients was analyzed by 13-color flow cytometry. Cryopreserved cells were incubated for 15 minutes at room temperature in PBS plus .5% BSA supplemented with 1 mg/mL total hIgG (Sanquin). Thereafter, cells were stained with 0.2 μg BV605- and BV711-labeled tetramers specific for the corresponding CMV or MiHA epitopes (Table 2) [4], and incubated for 30 minutes at room temperature. Then cells were labeled with the following antibodies: CD3-BV510 (UCHT1), CD8-PerCP (SK1), CD45RA-Alexa Fluor 700 (HI100), CCR7-PE-CF594 (150503), and CD56-BUV737 (NCAM16,2; all from BD Biosciences, San Jose, CA). For detecting costimulatory and coinhibitory molecules, the following antibodies were used: CD27-FITC (M-T271), ICOS-PE (DX29), CD28-PE-Cy7 (CD28.2), CD137-APC (4B4-1), CTLA-4-BV421 (BNI3), 2B4-PE (2-69), CD57-BV421 (NK-1), BTLA-PE (J168-540), and PD-1-BV421 (EH12.1), all from BD Biosciences; CD200R-FITC (380525), TIGIT-APC (741182), LAG-3-APC (polyclonal goat IgG), and IgG-APC, from R&D Systems (Minneapolis MN); OX-40-PE-Cy7 (BER-ACT35), TIM-3-PE-Cy7 (F38-2E2), IgG1-FITC, -PE, -APC, and -BV421 (MOPC-21), IgG2a-FITC, -PE, and -BV421 (MOPC-173), IgG2b-FITC, and -APC (MPC-11), from Biolegend (San Diego, CA); KLRG-1-FITC (REA261), from Miltenyi Biotec (Bergisch Gladbach, Germany), and IgG1-PE-Cy7 (679.1Mc7), from Beckman Coulter (Fullerton, CA). Cells were incubated for 30 minutes at 4°C and then washed with PBS. For live/dead discrimination, cells were then incubated for 30 minutes at 4°C with 1:1000 diluted Fixable Blue Dead Cell kit (Thermo Fisher Scientific, Waltham, MA). The panel design and laser alignment are summarized in Table S3. Cells were analyzed on a 5-laser FACSAria II cell sorter (BD Biosciences).

Data and Statistical Analysis

Flow cytometry data were analyzed using Kaluza version 1.5a (Beckman Coulter) or FlowJo version 10.2 (FlowJo, Ashland, OR). The gating strategy is depicted in detail in Figure S1. First, singlets and live cells were gated, then autofluorescence negative cells (using an unstained empty flow channel) were selected, and subsequently lymphocytes were gated using forward and side scatter. $CD4^+$ T cells were defined as $CD56^-CD3^+CD8^-$; $CD8^+$ T cells, as $CD56^-CD3^+CD8^+$. Within the $CD8^+$ T cell population, CMV- or MiHA-specific T cells were gated as positive for both tetramer-BV605 and tetramer-BV711. Furthermore, memory cell subsets were gated and defined as follows: $CCR7^+CD45RA^+$ naïve(-like) T cells (Tn), $CCR7^+CD45RA^-$ central memory T cells (Tcm), and $CCR7^-$ effector/effector memory T cells (Tem). Isotype-matched controls were used to evaluate the positivity for the cosignaling molecules; that is, each isotype gate was set at ≤1% positive. Tetramer-positive $CD8^+$ T cell populations were also analyzed using the bh-SNE algorithm in CYT version 2.0 from the Dana Pe'er Lab of Computational Systems Biology (New York, NY) and MATLAB (MathWorks, Natick, MA) [26]. In brief, the algorithm converts multidimensional data into bidimensional maps by first calculating a pairwise distance matrix for the high-dimensional space and then transforming it into a similarity matrix using a varying Gaussian kernel. A random bidimensional map is rendered, and pairwise similarities are calculated for the low-dimensional space created. The map is then optimized in iteration steps using the calculated similarity between any given 2 cells to optimally redistribute them on the map. Data quantifications were made in Prism version 5.03 (GraphPad Software, La Jolla, CA), SPICE version 5.3 (National Institute of Allergy and Infectious Diseases, Rockville, MD) and CIMminer (National Institutes of Health, Bethesda, MD) [27]. For a statistical comparison of SPICE pie charts, the built-in test in SPICE software was used, applying 1,000,000 permutations; as described by Roederer et al. [28] and Legat et al. [29]. For heatmap clustering analyses in CIMminer software with average linkage and the Pearson coefficient was used to determine the correlation between subset populations and expression of the different cosignaling molecules. Other P values were obtained using a 2-tailed t test or 1-way analysis of variance followed by a Bonferroni post hoc test as indicated, with $^*P < .05$, $^{**}P < .01$, and $^{***}P < .001$.

RESULTS

Distinct Coinhibitory Molecule Expression Profiles During T Cell Differentiation

To evaluate differences in T cell subset composition and expression profiles of cosignaling molecules, $CD4^+$ and $CD8^+$ T cells of healthy donors and allo-SCT recipients (at a median of 6 months after allo-SCT; range, 1-40 months) were analyzed by flow cytometry. Figure 1A shows representative flow cytometry plots of the $CD4^+$ and $CD8^+$ T cell subsets in a healthy donor and an allo-SCT recipient. The majority of both $CD4^+$ and $CD8^+$ T cells of allo-SCT recipients had a Tem phenotype ($CD4^+$, 65.3 ± 3.2%; $CD8^+$, 86.4 ± 1.6%), whereas these populations were substantially smaller in healthy donors ($CD4^+$, 29.8 ± 3.4%; $CD8^+$, 68.4 ± 4.0%; Figure 1B and Table S2). Of note, the $CD45RA^+CCR7^+$ T cell population of allo-SCT recipients contains both genuine naïve T cells and $CD95^+$ "naïve-like" or stem cell memory T cells, as we described previously [30]. Subsequently, we determined cosignaling molecule expression levels on $CD4^+$ and $CD8^+$ T cell memory subsets of healthy donors, and performed unsupervised clustering analyses (Figure 1C). Interestingly, for the $CD8^+$ T cells, perfect clustering of the different differentiation stages was observed based on distinct expression profiles of cosignaling

Table 1
Patient Characteristics

Patient	Disease	CMV Reactivation, mo after Allo-SCT	Antigen-Specific CD8+ T Cell Response (HLA Restriction)	Sampling Date, mo after Allo-SCT	DLI before Sampling Date, mo after Allo-SCT	Disease Status at Sampling Date	GVHD at Sampling Date	ISD at Sampling Date	Relapse, mo after Allo-SCT	Alive at Last FU, mo after Allo-SCT
1	MM	No	HA-1 (A2)	6	Yes, 6 (prophylactic)	CR	No	No	No	Yes, 86
2	NHL	No	SP110 (A3)	3	Yes, 2 (boost)	CR	Yes, aGVHD grade III	MMF, prednisone, etanercept, and inolimomab	No	
3	CML	No	HA-1 (A2)	6	Yes, 4 (prophylactic)	CR	Yes, aGVHD grade III	No	No	No, 15 (NRM)
4	MDS	No	HY (B7)	8	No	CR	Yes, cGVHD, extensive	No	No	Yes, 43
5	MDS	No	HA-1 (A2)	5	No	CR	No	Tacrolimus	No	Yes, 24
6	MDS	Yes, 8	HA-1 (A2)	11	Yes, 6 (prophylactic)	CR	Yes, cGVHD, extensive	CSA and prednisone	No	No, 49 (NRM)
7	AML	No	ARHGDIB (B7)	7	Yes, 6 (prophylactic)	CR	Yes, aGVHD grade I	CSA and prednisone	No	Yes, 151
8	AML	N.A.	HY (A2)	12	No	CR	No (resolved)	CSA	No	Yes, 199
9	AML	No	HA-1 (A2)	1	No	CR	No	CSA	No	Yes, 39
10	AML	Yes, 4	ARHGDIB (B7)	6	No	CR	Yes, cGVHD, extensive	CSA and prednisone	No	Yes, 39
11	AML	N.A.	HA-8 (A2)	6	No	CR	Yes, cGVHD, mild	CSA	No	Yes, 255
12	AML	N.A.	ARHGDIB (B7)	14	Yes, 8 (prophylactic)	CR	No	No	No	Yes, 145
13	MM	No	PANE (A3)	6	No	CR	Yes, cGVHD, mild	No	Yes, 9	No,10 (RRM)
14	NHL	No	HY (A2)	4	Yes, 4 (therapeutic)	Relapse	No	CSA	Yes, 3	No, 19 (RRM)
15	NHL	No	ARHGDIB (B7)	11	No	CR	No	No	Yes, 21	Yes, 250
16	CML	No	LRH-1 (B7)	14	Yes, 10 + 12 (therapeutic)	Relapse	No	No	Yes, 9	No, 75 (RRM)
17	AML	No	LRH-1 (B7)	40	Yes, 5 (prophylactic)	Relapse	No	No	Yes, 38 and 75	No, 94 (RRM)
18	AML	No	HY (A2)	3	No	CR	Yes, aGVHD, grade III	MMF	Yes, 10	No, 10 (RRM)
19	AML	No	HY (A2)	5	No	Relapse	No	No	Yes, 4	No, 5 (RRM)
20	AML	No	ARHGDIB (B7)	3	No	MRD	Yes, aGVHD, grade II	No	No	Yes, 32

FU indicates follow-up; NHL, non-Hodgkin lymphoma; CML, chronic myelogenous leukemia; AML, acute myelogenous leukemia; MM, multiple myeloma; MDS, myelodysplastic syndrome; Cy, cyclophosphamide; MRD, minimal residual disease; DLI, donor lymphocyte infusion; CR, complete remission; NA, not available; cGVHD, chronic graft-versus-host-disease; aGVHD, acute graft-versus-host-disease; ISD, immunosuppressive drugs; CSA, cyclosporin A; MMF, mycophenolic acid; RRM, relapse-related mortality; NRM, nonrelapse mortality.

Table 2
CMV- or MiHA-Specific Peptide Sequences Used for Tetramer-based Analysis of Antigen-Specific T Cell Populations

Antigen	HLA Restriction	Sequence
CMV	B7	RPHERNGFTVL
HA-1	A2	VLHDDLLEA
HA-8	A2	RTLDKVLEV
HY	A2	FIDSYICQV
PANE	A3	RVWDLPGVLK
SP110	A3	SLPRGTSTPK
ARHGDIB	B7	LPRACWREA
HY	B7	SPSVDKARAEL
LRH-1	B7	TPNQRQNVC

molecules. In case of the CD4+ T cells, the clustering was partial. As expected, CD27, CD28, and BTLA were highly expressed by naïve CD4+ and CD8+ T cells, and expression gradually decreased on T cell differentiation. In contrast, expression of KLRG-1, CD57, PD-1, and TIGIT was gained during T cell differentiation, with highest expression levels on Tem cells [29]. Of note, in allo-SCT recipients, clustering of T cell differentiation stages was also observed based on cosignaling expression profiles, despite differences in expression levels from healthy controls (data not shown).

We next investigated whether cosignaling molecules were differentially expressed by the different effector/memory T cell subsets of healthy donors compared with allo-SCT patients. The results are displayed for CD4+ T cells (Figure 2) and for CD8+ T cells (Figure 3). A slight decrease in CD28 expression on CD8+ T cells of allo-SCT recipients was observed compared with healthy donors. Furthermore, we detected increased OX-40 expression on the CD4+ Tcm and Tem cells of allo-SCT recipients, and elevated ICOS expression on the Tcm cells. Interestingly, KLRG-1 was expressed by the "naive-like" T cells, whereas PD-1 and CD57 expression was significantly higher on Tcm and Tem of both the CD4+ and CD8+ T cell populations in allo-SCT recipients. Collectively, these data indicate that the CD4+ and CD8+ T cell populations of allo-SCT recipients have distinct cosignaling molecule profiles that change during T cell differentiation, similar to those of healthy donors.

MiHA-Specific CD8+ T Cells Show an Early Differentiation Phenotype Accompanied with High Expression of Coinhibitory Molecules

We next examined the cosignaling molecule expression profiles on antigen-specific CD8+ T cells. We compared MiHA-specific CD8+ T cells with CMV-specific CD8+ T cells from healthy donors and allo-SCT recipients using a flow cytometry-based dual-color tetramer staining approach [4]. Figure 4A shows representative flow cytometry plots of CMV- and MiHA-specific CD8+ T cells and their respective effector/memory subset composition. Almost all CMV-specific CD8+ T cells from both healthy donors (84.6 ± 7.7%) and allo-SCT recipient (95.1 ± 1.3%) displayed a Tem phenotype, as did the MiHA-specific CD8+ T cells (91.9 ± 1.6%; Figure 4B and Table S1). Therefore, we compared the expression of cosignaling molecules on CMV- and MiHA-specific CD8+ T cells with the corresponding expression profiles of the total CD8+ Tem cell population of allo-SCT recipients (data for healthy donors are provided in Figure S2). The phenotype of MiHA-specific CD8+ T cells was found to differ significantly from that of the total CD8+ Tem population and CMV-specific CD8+ T cells based on augmented expression of CD27, CD28, CD278 (ICOS), and CD137 (4-1BB) (Figure 4C and D). In addition, we observed lower expression levels of KLRG-1 and CD57 on MiHA-specific CD8+ T cells, reflecting their early differentiation stage. Of note, along with lower expression of terminal differentiation markers and increased expression of the aforementioned costimulatory molecules, significantly elevated levels of PD-1, TIM-3, and TIGIT were observed as well. Findings were similar for percentage of positive cells and expression based on mean fluorescence intensity (data not shown). Taken together, these data indicate that MiHA-specific CD8+ T cells display a recently activated and early differentiation phenotype with high expression of PD-1, TIGIT, and TIM-3, which may be the result of activation-induced up-regulation [29], but also could reflect T cell exhaustion.

MiHA-Specific CD8+ T Cells Exhibit Distinctive Clustering Profiles with Increased Expression of Inhibitory and Stimulatory Receptors

Coexpression profiles of cosignaling molecules on antigen-specific CD8+ T cells of healthy donors and allo-SCT recipients were compared using different clustering analyses. First, tetramer-positive T cell populations were analyzed using the bh-SNE algorithm. Here analysis was performed separately for each flow cytometry panel, clustering individual CMV- or MiHA-specific CD8+ T cells based on the fluorescence intensities of the 5 cosignaling molecules in each panel (Figure 5A and Figure S3). Interestingly, MiHA-specific CD8+ T cells exhibited a distinct clustering pattern compared with CMV-reactive CD8+ T cells based on differential expression of CD27, CD28, and CD137 (panel 1; Figure S3A); high TIGIT and lack of CD57 (panel 2, Figure S3B); and high expression of PD-1, TIM-3, and BTLA and lack of KLRG-1 (panel 3, Figure S3C). Of note, the clustering patterns seen for the CMV-specific CD8+ T cells of healthy donors versus allo-SCT recipients were relatively similar (Figure 5A). These data were confirmed by unsupervised cluster analysis, displayed in a heatmap, where MiHA-specific CD8+ from allo-SCT recipients clustered together in a distinctive pattern compared with CMV-specific CD8+ T cells (Figure 5B). These differences could be attributed predominately to increased expression of costimulatory CD27 and CD28, collectively with elevated levels of coinhibitory PD-1, TIGIT, TIM-3, and BTLA on the MiHA-specific CD8+ T cells.

To look at these coexpression profiles from a different angle, we performed additional SPICE analysis. This analysis demonstrated that almost all of the MiHA-specific CD8+ T cells expressed CD27 and CD28 (Figure 5C). Furthermore, this population contained a higher proportion of cells triple-positive for CD27, CD28, and CD137 compared with CMV-specific CD8+ T cells, regardless of healthy donor or allo-SCT recipient origin. Furthermore, the MiHA-specific CD8+ T cell population showed lower expression of the terminal differentiation marker CD57 and contained a higher frequency of TIGIT+CD57− cells. Finally, MiHA-specific CD8+ T cells showed increased coexpression of PD-1, TIM-3, and BTLA, whereas lower KLRG-1 levels were observed compared with CMV-specific CD8+ T cells. Of note, in all 3 panels, MiHA-specific CD8+ T cells coexpressed significantly more cosignaling molecules than CMV-specific CD8+ T cells. This was especially striking in panel 3, where the average proportion of cells coexpressing ≥3 coinhibitory molecules was 57.2 ± 5.6% (SEM) for the MiHA-specific CD8+ T cells, versus only 25.1 ± 5.7% and 30.0 ± 6.6%, respectively, in CMV-specific CD8+ T cells of healthy donors and allo-SCT recipients. Taken together, these findings indicate that MiHA-specific CD8+ T cells exhibit distinctive clustering profiles, with an increased proportion of cells simultaneously expressing multiple coinhibitory

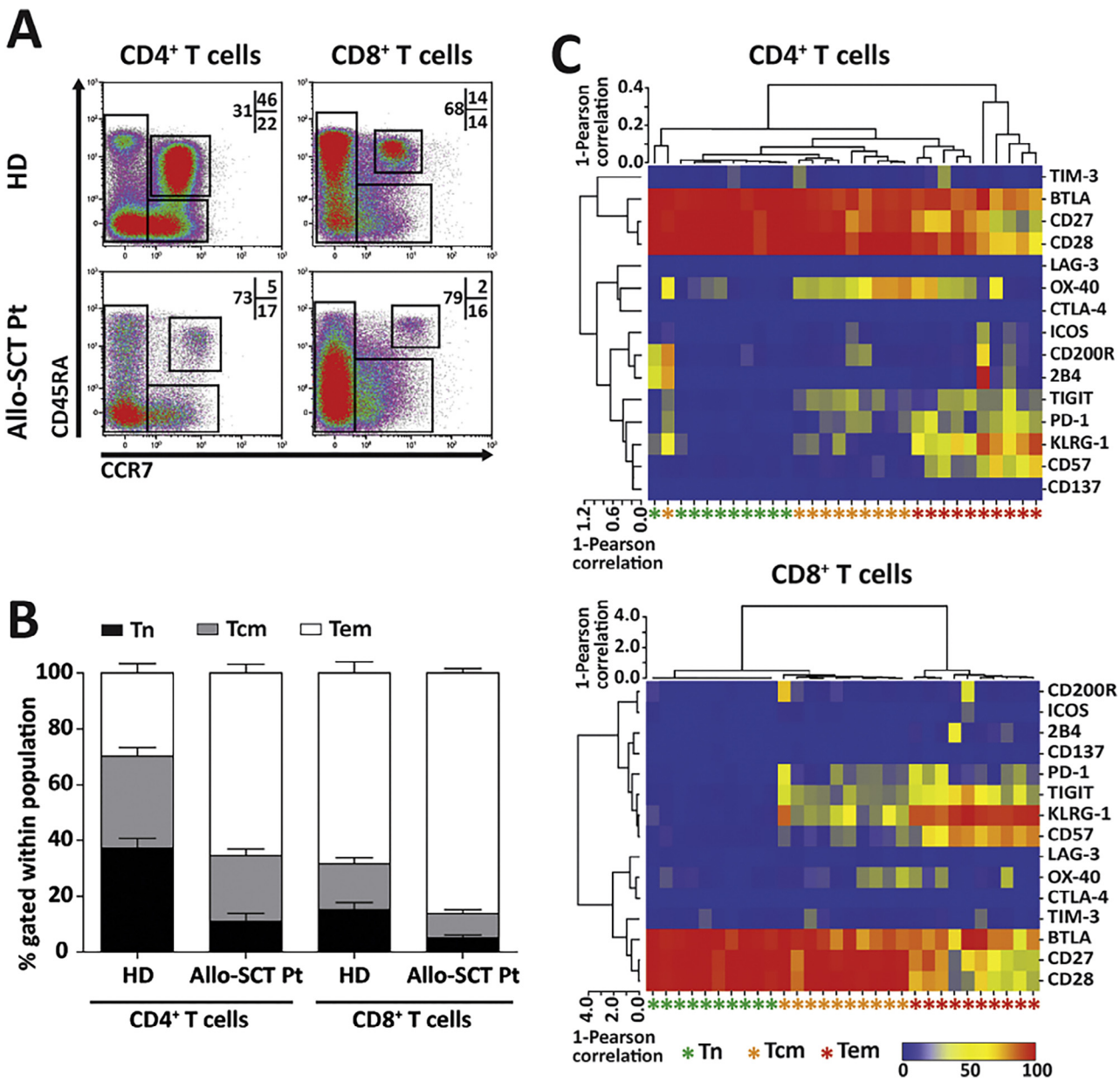

Figure 1. Cosignaling molecules show distinct coexpression profiles during T cell differentiation. CD4⁺ and CD8⁺ T cell subsets of healthy donors (HD) and allo-SCT recipients (allo-SCT patients) were examined for expression of coinhibitory and costimulatory molecules using flow cytometry. T cell differentiation stages were analyzed by gating on CD45RA and CCR7 expression. (A) Representative flow cytometry plots of the CD8⁺ and CD4⁺ subset composition in 1 HD and 1 allo-SCT pt (no. 3). (B) Combined data of CD4⁺ and CD8⁺ T cell subset composition for the HDs and allo-SCT recipients (HD: n = 10; allo-SCT pt: n = 30). Naïve/naïve-like T cells (Tn), CD45RA⁺CCR7⁺ (black); central memory T cells (Tcm), CD45RA⁻ CCR7⁺ (gray); effector memory T cells (Tem), CCR7⁻ (white). Data are shown as mean ± SEM for each subset as proportion of the CD4⁺ and CD8⁺ T cell populations. (C) Unsupervised clustering analysis with the Pearson coefficient was performed on cosignaling molecule expression levels on CD4⁺ and CD8⁺ T cells of HDs (n = 10). Data are shown in a heat map with a color code showing expression from 0% (blue) to 100% positivity (red) for the corresponding marker. Each row represents a different cosignaling molecule, and each column represents a T cell subset from 1 particular donor. Below the heat map, the classical differentiation stages based on CD45RA and CCR7 expression are indicated with a colored asterisk: green, Tn; orange, Tcm; red, Tem.

molecules, including PD-1, TIM-3, and TIGIT, as well as CD27 and CD28.

High Expression of OX-40, PD-1, TIGIT, and KLRG-1 on MiHA-Specific CD8⁺ T Cells Is Associated with Relapse in Allo-SCT Recipients

Finally, we evaluated whether distinct T cell expression signatures showed associations with clinical outcomes. To do so, we compared the expression of cosignaling molecules on MiHA-specific CD8⁺ T cells of patients remaining in remission (n = 12; patients 1-12) with those of patients with persistent or relapsed disease after allo-SCT (n = 8; patients 13-20). The median age at transplantation was 43 years (range, 28-58 years) for the relapsed patients versus 50 years (range, 26-63 years) in the remission group. Analyzed samples were obtained at a median of 11 months (range, 3-40 months) after allo-SCT for relapsed patients versus 7 months (range, 1-14 months) for nonrelapsed patients. At the time of analysis, 8 of 12 patients in remission were still being treated with immunosuppressive drugs, compared with 2 of 8 relapsed

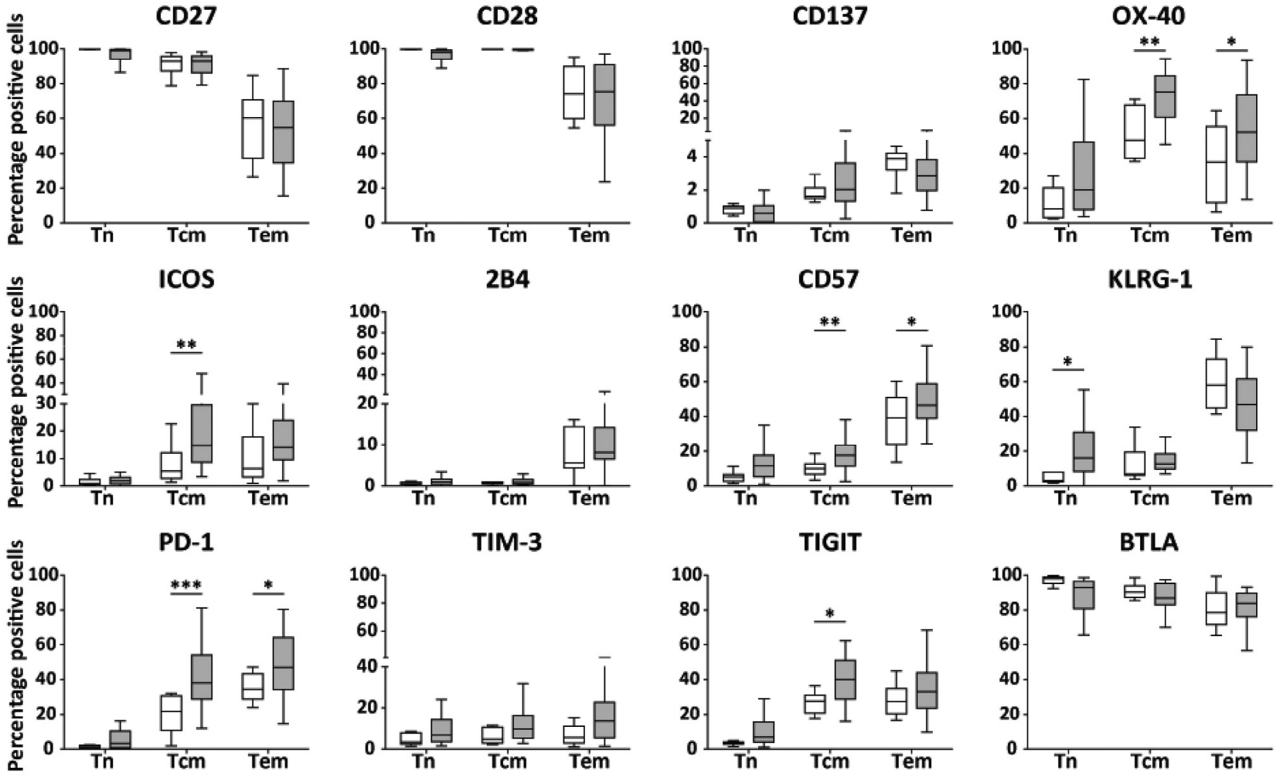

Figure 2. OX-40, ICOS, CD57, PD-1, and TIGIT are expressed at higher levels by CD4⁺ memory T cells of allo-SCT recipients. Expression of cosignaling molecules in the context of CD4⁺ T cell differentiation was analyzed using flow cytometry for healthy donors (HDs, white bars; n = 10) and allo-SCT recipients (allo-SCT pts, gray bars; n = 30). Statistical analysis was performed using a 2-tailed *t* test. $^{*}P < .05$; $^{**}P < .01$; $^{***}P < .001$.

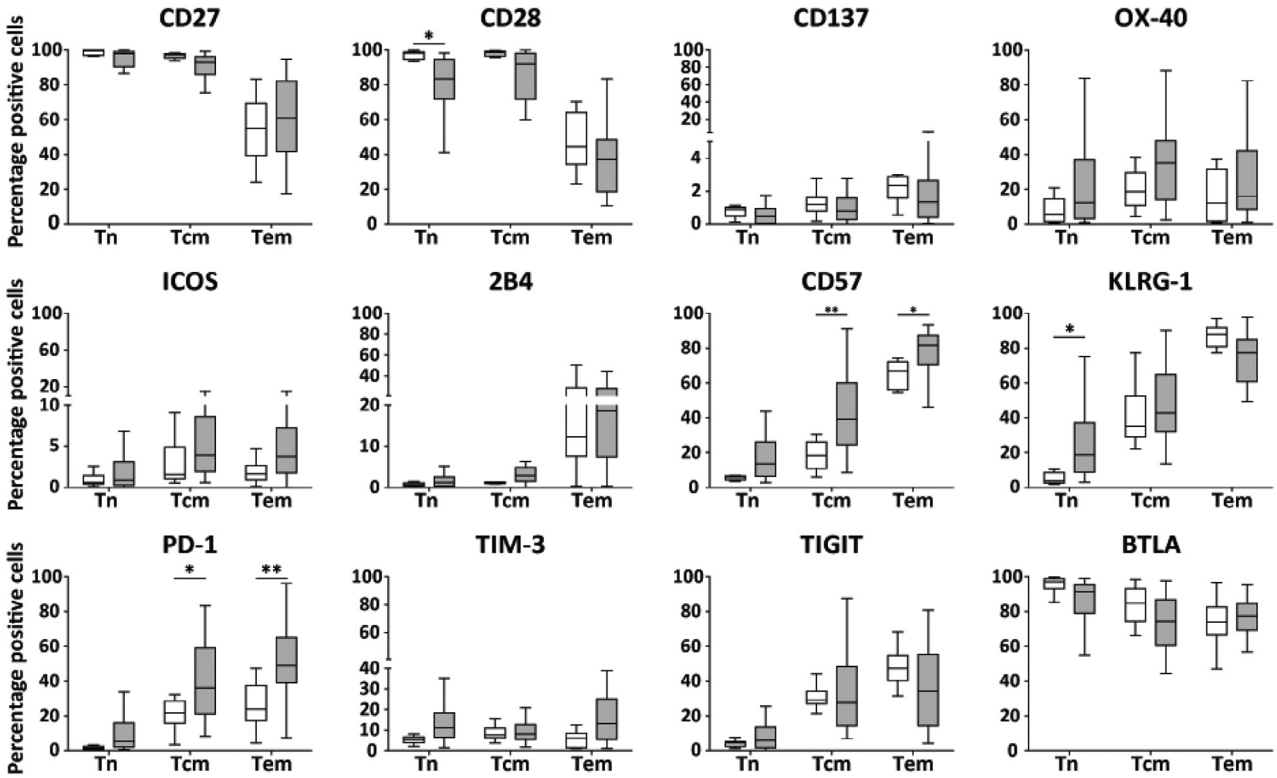

Figure 3. PD-1 and CD57 are highly expressed by CD8⁺ memory T cells of allo-SCT recipients. Expression of cosignaling molecules in the context of CD8⁺ T cell differentiation was analyzed by flow cytometry for healthy donors (HDs, white bars; n = 10) and allo-SCT recipients (allo-SCT pts, gray bars; n = 30). Statistical analysis was performed using a 2-tailed *t* test. $^{*}P < .05$; $^{**}P < .01$; $^{***}P < .001$.

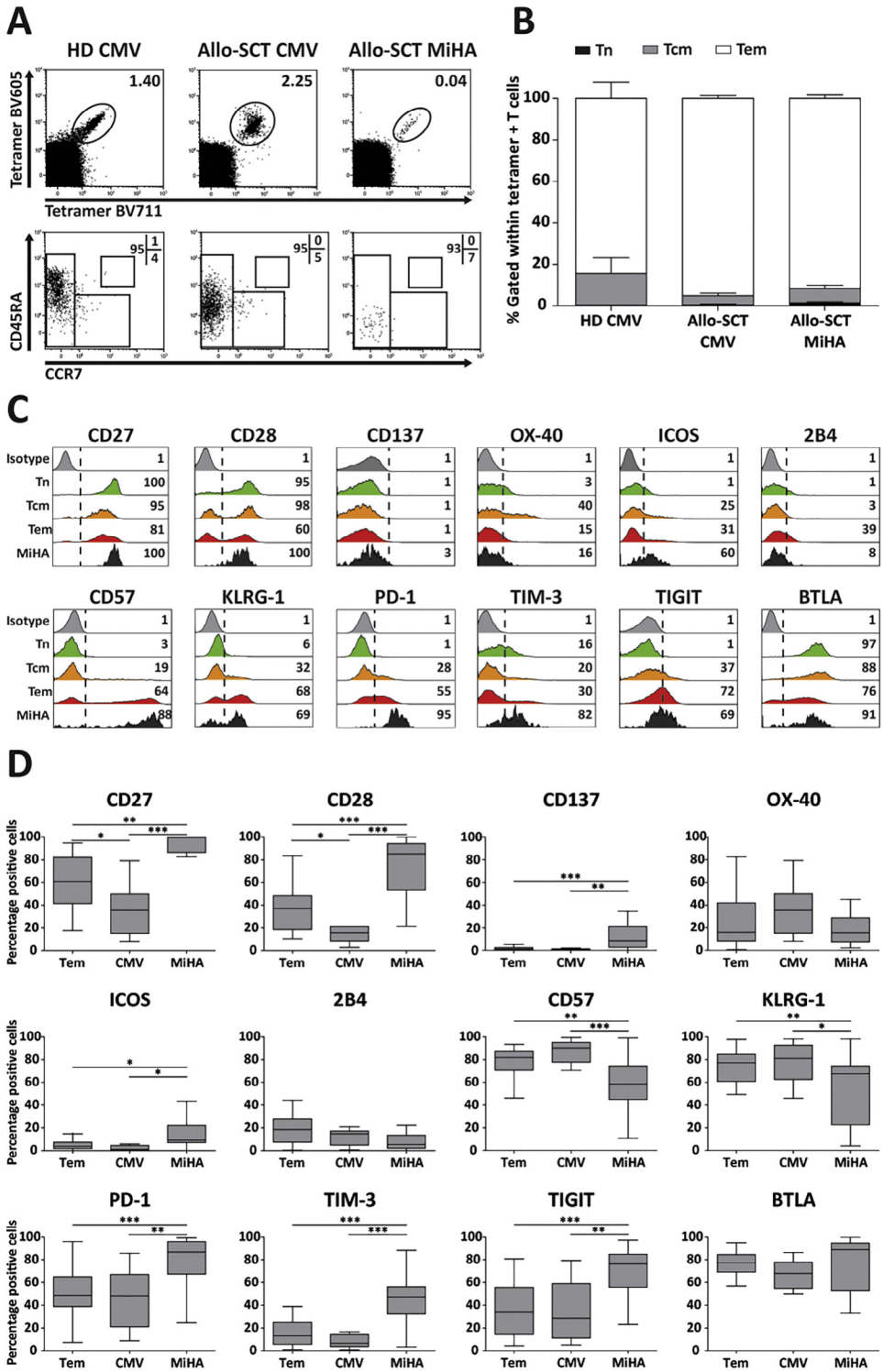

Figure 4. MiHA-specific CD8⁺ T cells exhibit an early differentiation phenotype accompanied with high expression of coinhibitory molecules. Antigen-specific CD8⁺ T cells of healthy donors (HDs) and allo-SCT recipients (allo-SCT patients) were examined for expression of coinhibitory and costimulatory molecules using dual-color tetramer-based flow cytometry. (A) Representative plots of CMV- and MiHA-specific CD8⁺ T cells and their respective differentiation stage are shown for 1 HD and 1 allo-SCT pt (no. 24) with a detectable CMV-specific CD8⁺ T cell response, and 1 allo-SCT pt (no. 15) with a detectable MiHA-specific CD8⁺ T cell response. The number in the plots indicates the percentage of MiHA-specific CD8⁺ T cells positive for both tetramers. (B) Combined data of the subset composition within the antigen-specific CD8⁺ T cell population are shown (HD, n = 10; allo-SCT pt CMV, n = 10; allo-SCT pt MiHA, n = 20). Naïve-like T cells (Tn), CD45RA⁺CCR7⁺ (black); central memory T cells (Tcm), CD45RA⁻ CCR7⁺ (gray); effector memory T cells (Tem), CCR7⁻ (white). Data are expressed as mean ± SEM for each subset as proportion of the antigen-specific CD8⁺ T cell populations. (C) Surface expression of the different cosignaling molecules is shown for the MiHA-specific CD8⁺ T cell population (black) and CD8⁺ T cell subsets of 1 allo-SCT pt (no. 7) (Tn, green; Tcm, orange; Tem, red), compared with the corresponding isotype control staining (gray). Dotted lines represent gates set at <1% positive for the isotype control, and the numbers in the plots represent the percentage of cells positive for the respective receptor. (D) Combined data showing the percentage of cells positive for each cosignaling molecule within the total CD8⁺ Tem versus CMV- and MiHA-specific CD8⁺ T cell populations of allo-SCT pt (allo-SCT pt Tem, n = 30; allo-SCT pt CMV, n = 10; allo-SCT pt MiHA, n = 20). Statistical analysis was performed using 1-way analysis of variance followed by a Bonferroni post hoc test.*$P < .05$; **$P < .01$; ***$P < .001$.

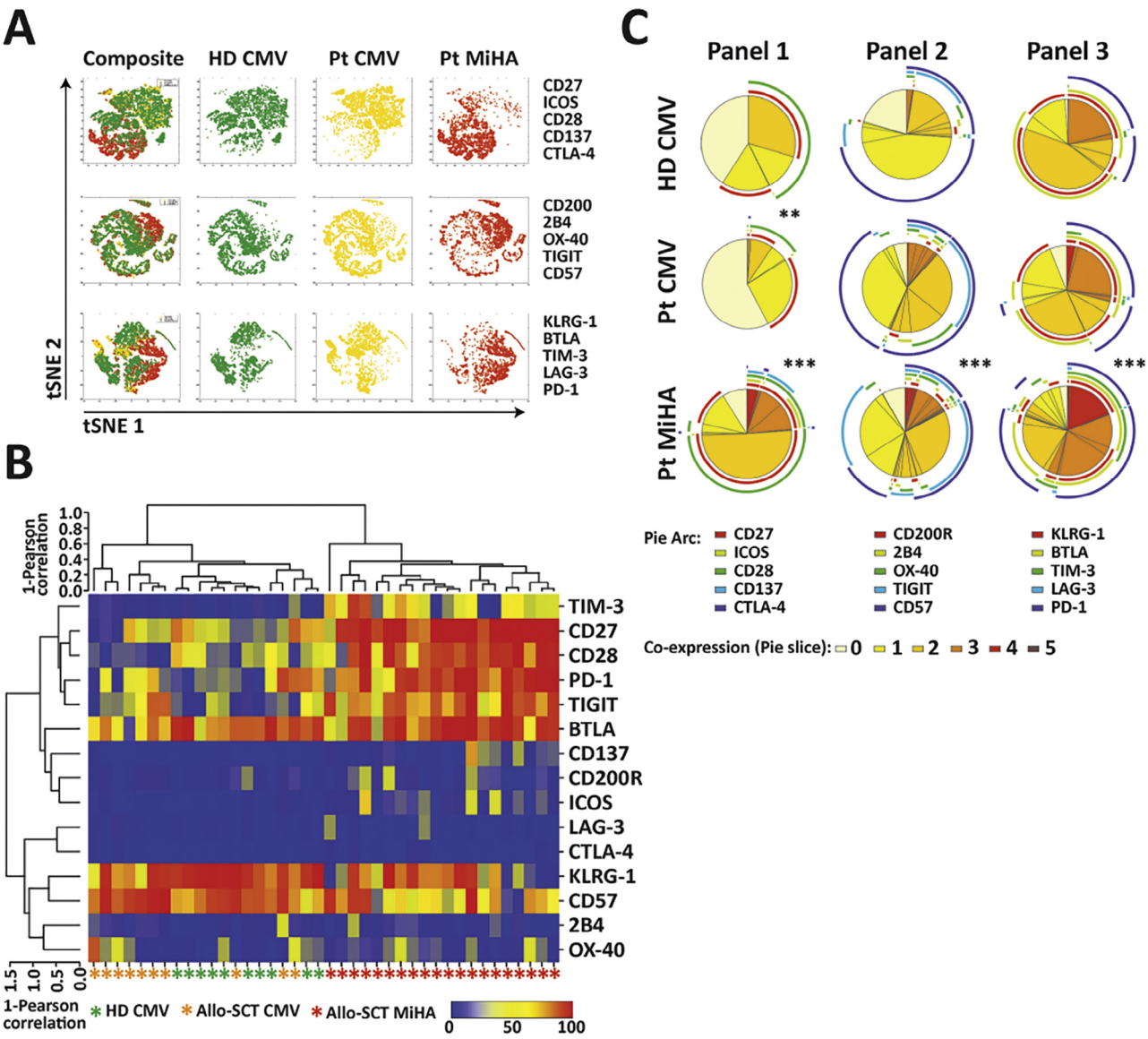

Figure 5. MiHA-specific CD8⁺ T cells have a distinct coexpression profile with high expression of inhibitory and stimulatory receptors. Antigen-specific CD8⁺ T cells of healthy donors (HDs) and allo-SCT recipients (allo-SCT pts) were examined for expression of coinhibitory and costimulatory molecules by flow cytometry using 3 different panels. CMV- and MiHA-specific CD8⁺ T cells were gated based on dual-color tetramer staining. (A) bh-SNE clustering analysis was performed for each flow cytometry panel, containing 5 antibodies against different cosignaling molecules. Composite overlays (*left*) and individual maps (*right*) visualize the clustering signatures of HD CMV (green), allo-SCT pt CMV (yellow), and allo-SCT pt MiHA (red). (B) Unsupervised average linkage analysis was performed with the Pearson coefficient for each antigen-specific CD8⁺ T cell population, and is displayed in a heat map. The color scale indicates expression from 0% (blue) to 100% positivity (red) for the corresponding marker. Each row represents a different cosignaling molecule, and each column represents a different individual. Below the heat map, the donor population and corresponding antigen specificities are indicated with colored asterisks: green, HD CMV; orange, allo-SCT Pt CMV; red, allo-SCT MiHA Pt. (C) Coexpression patterns were determined with SPICE software. The pies depict the average proportion of cells expressing 0 to 5 of the cosignaling molecules, and the arcs indicate which markers are expressed by the corresponding pies. Statistical differences were analyzed using the built-in statistical tool. $^{*}P < .05$; $^{**}P < .01$; $^{***}P < .001$. HD CMV, n = 10; allo-SCT Pt CMV, n = 10; allo-SCT Pt MiHA, n = 20.

patients. This corresponds with the higher rate of graft-versus-host disease (GVHD) in the remission group (7 of 12) versus the relapse group (3 of 8). There were no differences in donor lymphocyte infusion administration between the patient groups. Of note, none of the patients with a MiHA-specific CD8⁺ T cell response had detectable CMV disease at the sampling date.

We found significantly higher expression of OX-40, KLRG-1, PD-1, and TIGIT on MiHA-specific CD8⁺ T cells of allo-SCT recipients who relapsed (Figure 6A). The other cosignaling molecules were not differentially expressed and did not exhibit any differences in coexpression patterns (Figure 6A and Figure S4). Observations were similar for percentage positive cells and expression based on mean fluorescence intensity (data not shown). To further demonstrate that coexpression of OX-40, KLRG-1, PD-1, and TIGIT defined a distinct T cell signature in patients who relapsed after allo-SCT, we established a new panel dedicated to these 4 receptors and remeasured MiHA-specific CD8⁺ T cells of 9 patients with mostly myelogenous malignancies (remission patients: 5, 8, 9, 11 and 12; relapse patients: 15, 17, 19, and 20) (Figure 6B). Interestingly, the relapsed patients had a small subset of quadruple-positive

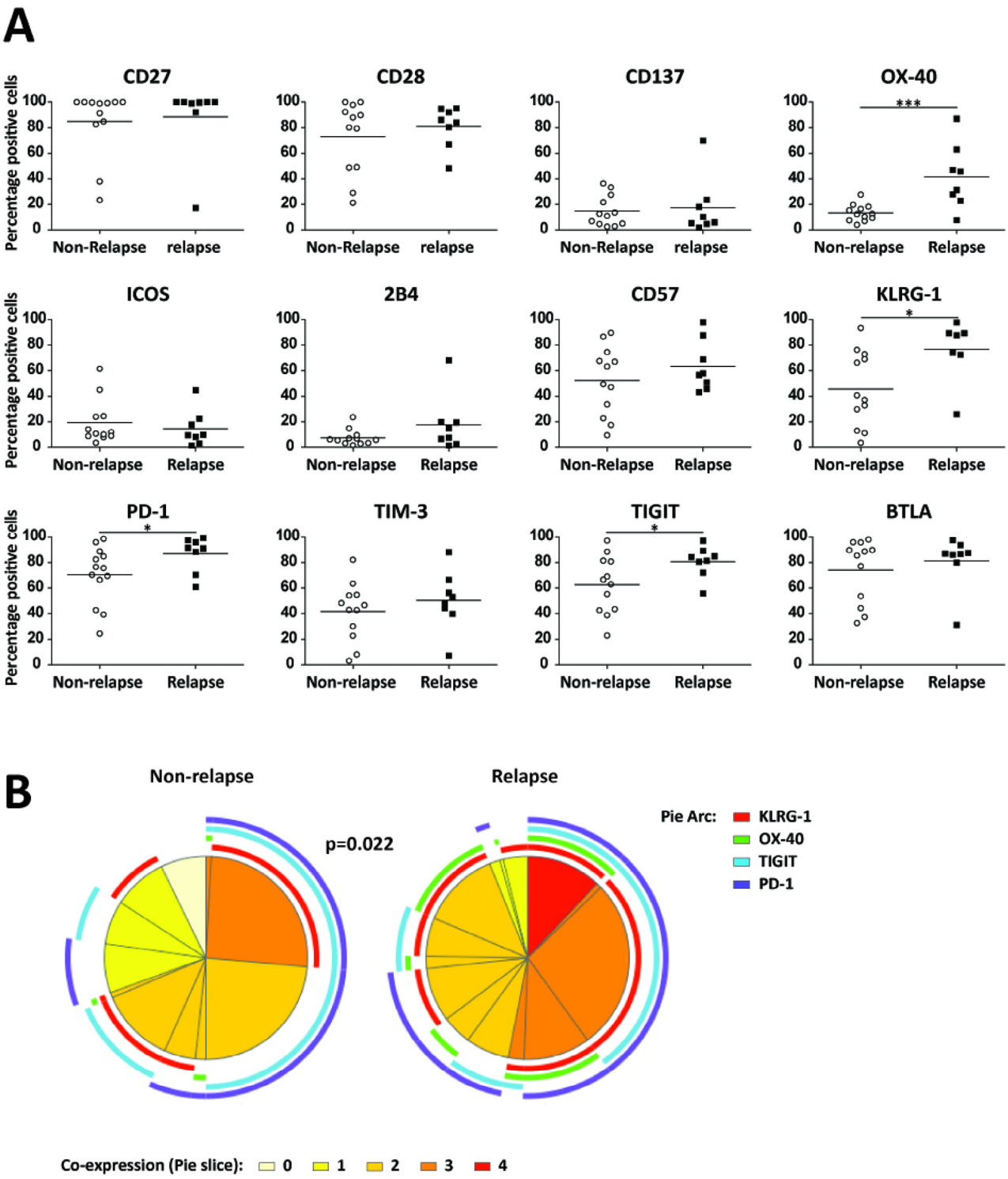

Figure 6. High expression of PD-1, TIGIT, OX-40, and KLRG-1 on MiHA-specific CD8⁺ T cells is associated with relapse in allo-SCT recipients. Expression levels of cosignaling molecules on MiHA-specific CD8⁺ T cells of allo-SCT recipients (allo-SCT pts) were evaluated using flow cytometry and analyzed in the context of relapse post-transplantation. (A) For each receptor, the percentage of positive cells was determined within the MiHA-specific CD8⁺ T cell populations of nonrelapsed patients (n = 12; open circles) and relapsed patients (n = 8; black solid squares). Lines indicate the mean. Statistical analysis was performed using a 2-tailed *t* test. **P* < .05; ****P* < .001. (B) Coexpression profiles of a dedicated panel specific for the 4 receptors that were significantly differentially expressed in nonrelapsed versus relapsed allo-SCT recipients were examined with flow cytometry and analyzed using SPICE software. The pie charts depict the average proportion of cells expressing 0 to 4 of the cosignaling molecules, and the arcs indicate whether KLRG-1 (red), OX-40 (green), TIGIT (light blue), and/or PD-1 (dark blue) is expressed by the corresponding pies. Statistical differences were analyzed using the built-in statistical tool.

MiHA-specific CD8+ T cells that was not found in the remission patient group. Furthermore, in the relapsed patients, a larger proportion of the MiHA-specific CD8+ T cells was triple-positive. The expression of OX-40 and TIGIT seemed mutually exclusive. Importantly, this expression signature was independent of treatment with immunosuppressive drugs and GVHD occurrence (data not shown). To conclude, our explorative studies show that MiHA-specific T cells of relapsed patients exhibit a distinct phenotype characterized by enhanced coexpression of PD-1, TIGIT, and KLRG-1. This expression signature may be the result of T cell activation or may reflect T cell dysfunction due to continuous antigen encounter. Treatment with novel combinations of antagonistic and agonistic antibodies would be an attractive strategy to boost the potency of these T cells to treat relapse after allo-SCT.

DISCUSSION

The involvement of cosignaling molecules in tumor immune escape mechanisms has become increasingly evident in recent years. The impressive results achieved in clinical trials blocking the PD-1/PD-L1 axis in solid and hematologic malignancies [15] illustrate the potent effects of releasing the coinhibitory "breaks" on reinvigoration of antitumor immunity. Dysfunctional T cells can simultaneously express multiple coinhibitory receptors, and subsequent signaling can contribute to their dysfunctional state. Interestingly, combined blockade of CTLA-4 and PD-1 resulted in additive or even synergistic clinical efficacy in cancer patients [24,31]. In addition to CTLA-4 and PD-1, novel cosignaling molecules are now being investigated, including BTLA, LAG-3, TIM-3, and TIGIT [8-11,32]. We previously reported the involvement of PD-1 and BTLA signaling in suppressing MiHA-specific CD8+ T cell functionality, which could be alleviated by antibody-mediated blockade in vitro [13]. However, not all patients respond to single antibody therapy, which may reflect differences in the dominance of immunosuppressive mechanisms used by the tumor [13,15-17]. This emphasizes the need for new immunotherapeutic strategies targeting novel combinations of coinhibitory molecules, and potentially also costimulatory receptors, to boost tumor-reactive T cell responses. The aim of this study was to identify (co)expression profiles of a comprehensive set of cosignaling molecules on MiHA-specific CD8+ T cells in relation to clinical outcome after allo-SCT. Major challenges of multicolor flow cytometry include the complex data analyses and limitations of 2D data visualization. Here we analyzed our data extensively through unsupervised clustering, bh-SNE, and SPICE analyses to elucidate potential expression signatures associated with clinical outcomes.

We used a well-established T cell effector/memory subset definition based on CD45RA and CCR7 expression [33] to evaluate the expression patterns of 15 cosignaling molecules during T cell differentiation using unsupervised clustering analysis. Interestingly, Tn, Tcm, and Tem clustered perfectly together for the CD8+ T cells based on defined cosignaling molecule expression patterns. Partial clustering was observed for the CD4+ T cell subsets. These data illustrate the importance of evaluating cosignaling molecule expression profiles in the context of T cell differentiation. In accordance with this, others also have reported that changes in the expression of CD27, CD28, BTLA, KLRG-1 and CD57 are correlated with T cell differentiation stages [29,34]. Here we analyzed CD4+ and CD8+ T cell subsets of healthy donors versus allo-SCT recipients. We observed that allo-SCT recipients had significantly higher expression of PD-1 and CD57 on CD4+ and CD8+ Tcm and Tem populations, and increased levels of OX-40 in Tcm and Tem CD4+ T cells. These data support that T cells of allo-SCT recipients exhibit a highly activated/terminally differentiated phenotype [35]. These observations likely can be attributed to inflammation caused by the conditioning regimen [36], viral reactivation, development of antiviral and alloreactive immune responses, and occurrence of GVHD [37,38].

We next studied the (co)expression patterns of cosignaling molecules on MiHA-specific CD8+ T cells, because these target highly immunogenic antigens expressed by hematologic tumor cells. CMV-reactive CD8+ T cells served as controls for MiHA-specific CD8+ T cells. We identified increased expression levels of multiple coinhibitory molecules, including PD-1, TIM-3, and TIGIT, on MiHA-specific CD8+ T cells, whereas these T cells retained an early differentiation phenotype with lower CD57 and KLRG1 and high CD27 and CD28 expression. The distinctive phenotype of the MiHA-specific CD8+ T cells compared with CMV-specific CD8+ T cells was also confirmed with bh-SNE analysis and unsupervised clustering analysis and could be attributed to increased expression levels of PD-1, TIGIT, TIM-3, BTLA, CD27, and CD28. Notably, a larger proportion of MiHA-specific CD8+ T cells simultaneously expressed multiple cosignaling molecules at their cell surface compared with CMV-specific CD8+ T cells. High expression of coinhibitory molecules, such as PD-1, TIM-3, and TIGIT, by tumor-reactive T cells can reflect T cell activation, but also may be a hallmark of functional impairment [8,9,18-22]. Although individual expression of coinhibitory receptors is not selective or indicative of exhaustion, simultaneous expression of multiple coinhibitory receptors is a key feature of T cell dysfunction in cancer and chronic viral infections [10,11,35]. These coexpression patterns are mechanistically relevant, because these receptors can act together in impairing T cell function. Simultaneous blockade of multiple coinhibitory molecules can result in synergistic reversal of T cell dysfunction, as has been demonstrated for PD-1 and TIM-3 and for PD-1 and TIGIT [21,32,35].

Most importantly, we analyzed the phenotype of MiHA-specific CD8+ T cells in relation to clinical outcome. MiHA-specific CD8+ T cells of patients who relapsed showed increased expression of PD-1, TIGIT, OX-40, and KLRG-1. This is in accordance with the results published by Schnorfeil et al. [39], who reported increased PD-1 expression on total CD8+ T cells to correlate with relapse. Similarly, Kong et al. [40] reported the association of high PD-1 and TIM-3 coexpression with leukemia relapse in patients with acute myelogenous leukemia after allo-SCT. In addition, TIGIT was found to be associated with CD8+ T cell exhaustion and poor clinical outcome in acute myelogenous leukemia [14]. Furthermore, up-regulation of the costimulatory molecules OX-40 and 4-1BB was observed on dysfunctional CD8+ TIL in human and murine melanoma [41,42]. Interestingly, in our analyses, approximately 10% of the T cells simultaneously expressed the 4 markers PD-1, TIGIT, OX-40, and KLRG-1, although TIGIT and OX-40 seemed mutually exclusive on the other MiHA-specific CD8+ T cells. On average, more than one-half of the cells were positive for ≥3 of these markers in the relapsed group. In contrast, only ~25% of the MiHA-specific CD8+ T cells were triple-positive in patients who remained in remission. Notably, this expression signature was independent of the type of MiHA-specific CD8+ T cell response, CMV reactivation, treatment with immunosuppressive drugs, and GVHD

occurrence. In the future, this signature may potentially be used for monitoring after allo-SCT.

This study has some limitations that should be addressed. Owing to limited availability of material, it was not possible to include more patients, select patients with a similar malignancy and/or MiHA-specific T cell response, use samples obtained at fixed time points after allo-SCT, or study kinetics of checkpoint profiles. Malignant cell intrinsic factors might have differentially altered coexpression profiles of checkpoint molecules on MiHA-specific CD8$^+$ T cells. In addition, the local tumor microenvironment may play a significant role in modulating T cell phenotype and functionality. Therefore, in the analyses with the dedicated PD-1, TIGIT, OX-40, and KLRG-1 panel, mostly MiHA-specific CD8$^+$ T cells of patients with myeloid malignancies were examined (7 with acute myelogenous leukemia, 1 with myelodysplastic syndrome, 1 with non-Hodgkin lymphoma). Future studies in larger, more homogenous cohorts are warranted to validate our findings and further elucidate the functional consequences and clinical importance of the expression signatures described in this explorative study.

Combined targeting of PD-1, TIGIT, OX-40, and KLRG-1 may allow tailored tuning of the type and magnitude of the tumor-reactive T cell responses. In previous ex vivo studies, we demonstrated that PD-1- and BTLA-expressing MiHA-reactive T cells respond to PD-1 and/or BTLA blockade, with the most pronounced effects observed for patients who relapsed after allo-SCT [12]. In addition to enhanced signaling via coinhibitory molecules, it has become clear that desensitization of costimulatory molecule signaling through the loss of adaptor molecules is another mechanism that can contribute to T cell dysfunction [43]. This indicates that both costimulatory and coinhibitory receptors are appealing targets for parallel agonistic and antagonistic antibody treatment. In solid cancers, monotherapy with antagonistic or agonistic antibodies targeting PD-1, TIGIT, or OX-40 has shown promising results [20]. Importantly, CTLA-4 and PD-1/PD-L1 blockade are now established treatment options for multiple solid cancers, and combination therapy with anti-TIGIT and/or anti-OX-40 is emerging [20,21,35,44]. Chauvin et al. [35] reported that dual blockade of TIGIT and PD-1 potently augmented antitumor CD8$^+$ T cell responses, as indicated by increased proliferation, cytokine production, and degranulation in vitro. Furthermore, OX-40 agonistic antibody treatment has been reported to promote proliferation and survival of activated CD8$^+$ T cells [45,46]. The crux of allo-SCT is the separation of GVT and GVHD reactivity. Systemic release of the immune brakes (checkpoints) may lead to induction and/or aggravation of GVHD in these patients. Recent studies on CTLA-4 and PD-1 blockade in patients with relapsed acute myelogenous leukemia and Hodgkin lymphoma after allo-SCT showed beneficial GVT responses, but also raised concerns about GVHD [47-56]. There are a few important caveats, however. Interestingly, in the study by Haverkos et al. [56], none of the patients treated with a haploidentical HLA-mismatched transplant developed GVHD after anti-PD-1 treatment. All 4 patients received post-transplantation cyclophosphamide in addition to calcineurin inhibitor as GVHD prevention. Thus, it is possible that incidence of GVHD after checkpoint inhibitors administration may vary depending on the type of GVHD prophylaxis. Further clinical studies are warranted to establish guidelines for checkpoint interference after allo-SCT. Alternatively, novel strategies for local interference with checkpoint signaling pathways in the tumor microenvironment, for instance, using targeted siRNA nanoparticles, might hold the key to boost GVT immunity without inducing and/or aggravating GVHD after allo-SCT.

In conclusion, we have shown that MiHA-specific CD8$^+$ T cells have a distinctive cosignaling molecule expression profile compared with CMV-reactive CD8$^+$ T cells. MiHA-specific CD8$^+$ T cells highly express the inhibitory receptors PD-1, TIGIT, and TIM-3, as well as the stimulatory receptors CD27 and CD28, while having a recently activated early differentiation phenotype based on low KLRG-1 and CD57, accompanied by CD137 positivity. Most importantly, high coexpression of PD-1, TIGIT, and KLRG-1 on MiHA-reactive CD8$^+$ T cells was associated with relapse after allo-SCT. Taken together, these data suggest that multiple cosignaling molecules may act together in regulating T cell-mediated tumor control. Treatment with antibodies targeting different cosignaling molecules would be an attractive adjuvant treatment strategy to boost the potency of these highly activated, potentially dysfunctional, tumor-reactive T cells to treat relapse after allo-SCT.

ACKNOWLEDGMENTS

The authors thank Jesse Oomen for technical assistance.

Financial disclosure: This work was supported by grants from the Dutch Cancer Society (KUN 2012-5410 and KUN 2011-5041).

Conflict of interest statement: There are no conflicts of interest to report.

Authorship statement: T.J.A.H. and W.J.N. designed and performed experiments and contributed to the writing of the paper; S.B. performed the bh-SNE analysis; R.W., R.C.W. and F.M. performed experiments; M.K. and J.H.F.F. provided essential materials and advice; L.L., J.H.J. and N.S. provided essential advice; and H.D. and W.H. designed the study and revised the manuscript. All authors contributed to manuscript revision.

SUPPLEMENTARY DATA

Supplementary data related to this article can be found online at doi:10.1016/j.bbmt.2017.11.027.

REFERENCES

1. Jenq RR, van den Brink MR. Allogeneic haematopoietic stem cell transplantation: individualized stem cell and immune therapy of cancer. *Nat Rev Cancer*. 2010;10:213-221.
2. Riddell SR, Berger C, Murata M, Randolph S, Warren EH. The graft-versus-leukemia response after allogeneic hematopoietic stem cell transplantation. *Blood Rev*. 2003;17:153-162.
3. van Bergen CA, van Luxemburg-Heijs SA, de Wreede LC, et al. Selective graft-versus-leukemia depends on magnitude and diversity of the alloreactive T cell response. *J Clin Invest*. 2017;127:517-529.
4. Hobo W, Broen K, van der Velden WJ, et al. Association of disparities in known minor histocompatibility antigens with relapse-free survival and graft-versus-host disease after allogeneic stem cell transplantation. *Biol Blood Marrow Transplant*. 2013;19:274-282.
5. D'Cruz LM, Rubinstein MP, Goldrath AW. Surviving the crash: transitioning from effector to memory CD8$^+$ T cell. *Semin Immunol*. 2009;21:92-98.
6. Norde WJ, Overes IM, Maas F, et al. Myeloid leukemic progenitor cells can be specifically targeted by minor histocompatibility antigen LRH-1-reactive cytotoxic T cells. *Blood*. 2009;113:2312-2323.
7. Wang X, Teng F, Kong L, Yu J. PD-L1 expression in human cancers and its association with clinical outcomes. *Onco Targets Ther*. 2016;9:5023-5039.
8. Woo SR, Turnis ME, Goldberg MV, et al. Immune inhibitory molecules LAG-3 and PD-1 synergistically regulate T-cell function to promote tumoral immune escape. *Cancer Res*. 2012;72:917-927.
9. Blackburn SD, Shin H, Haining WN, et al. Coregulation of CD8$^+$ T cell exhaustion by multiple inhibitory receptors during chronic viral infection. *Nat Immunol*. 2009;10:29-37.
10. Matsuzaki J, Gnjatic S, Mhawech-Fauceglia P, et al. Tumor-infiltrating NY-ESO-1-specific CD8$^+$ T cells are negatively regulated by LAG-3 and PD-1 in human ovarian cancer. *Proc Natl Acad Sci U S A*. 2010;107:7875-7880.

11. Fourcade J, Sun Z, Pagliano O, et al. PD-1 and Tim-3 regulate the expansion of tumor antigen-specific CD8(+) T cells induced by melanoma vaccines. *Cancer Res*. 2014;74:1045-1055.
12. Norde WJ, Maas F, Hobo W, et al. PD-1/PD-L1 interactions contribute to functional T-cell impairment in patients who relapse with cancer after allogeneic stem cell transplantation. *Cancer Res*. 2011;71:5111-5122.
13. Hobo W, Norde WJ, Schaap N, et al. B and T lymphocyte attenuator mediates inhibition of tumor-reactive $CD8^+$ T cells in patients after allogeneic stem cell transplantation. *J Immunol*. 2012;189:39-49.
14. Kong Y, Zhu L, Schell TD, et al. T-cell immunoglobulin and ITIM domain (TIGIT) associates with $CD8^+$ T-cell exhaustion and poor clinical outcome in AML patients. *Clin Cancer Res*. 2016;22:3057-3066.
15. Ansell SM, Lesokhin AM, Borrello I, et al. PD-1 blockade with nivolumab in relapsed or refractory Hodgkin's lymphoma. *N Engl J Med*. 2015;372:311-319.
16. Callahan MK, Postow MA, Wolchok JD. Targeting T cell co-receptors for cancer therapy. *Immunity*. 2016;44:1069-1078.
17. Sledzinska A, Menger L, Bergerhoff K, Peggs KS, Quezada SA. Negative immune checkpoints on T lymphocytes and their relevance to cancer immunotherapy. *Mol Oncol*. 2015;9:1936-1965.
18. Gagliani N, Magnani CF, Huber S, et al. Coexpression of CD49b and LAG-3 identifies human and mouse T regulatory type 1 cells. *Nat Med*. 2013;19:739-746.
19. Le Mercier I, Lines JL, Noelle RJ. Beyond CTLA-4 and PD-1, the generation Z of negative checkpoint regulators. *Front Immunol*. 2015;6:418.
20. Guo Z, Wang X, Cheng D, Xia Z, Luan M, Zhang S. PD-1 blockade and OX40 triggering synergistically protects against tumor growth in a murine model of ovarian cancer. *PLoS One*. 2014;9:e89350.
21. Johnston RJ, Comps-Agrar L, Hackney J, et al. The immunoreceptor TIGIT regulates antitumor and antiviral CD8(+) T cell effector function. *Cancer Cell*. 2014;26:923-937.
22. Anderson AC. Tim-3: an emerging target in the cancer immunotherapy landscape. *Cancer Immunol Res*. 2014;2:393-398.
23. Zarour HM. Reversing T-cell dysfunction and exhaustion in cancer. *Clin Cancer Res*. 2016;22:1856-1864.
24. Wolchok JD, Kluger H, Callahan MK, et al. Nivolumab plus ipilimumab in advanced melanoma. *N Engl J Med*. 2013;369:122-133.
25. Spierings E, Drabbels J, Hendriks M, et al. A uniform genomic minor histocompatibility antigen typing methodology and database designed to facilitate clinical applications. *PLoS One*. 2006;1:e42.
26. Amir ED, Davis KL, Tadmor MD, et al. viSNE enables visualization of high dimensional single-cell data and reveals phenotypic heterogeneity of leukemia. *Nat Biotechnol*. 2013;31:545-552.
27. Weinstein JN, Myers TG, O'Connor PM, et al. An information-intensive approach to the molecular pharmacology of cancer. *Science*. 1997;275:343-349.
28. Roederer M, Nozzi JL, Nason MC. SPICE: exploration and analysis of post-cytometric complex multivariate datasets. *Cytometry A*. 2011;79:167-174.
29. Legat A, Speiser DE, Pircher H, Zehn D, Fuertes Marraco SA. Inhibitory receptor expression depends more dominantly on differentiation and activation than "exhaustion" of human CD8 T cells. *Front Immunol*. 2013;4:455.
30. van der Waart AB, van de Weem NM, Maas F, et al. Inhibition of Akt signaling promotes the generation of superior tumor-reactive T cells for adoptive immunotherapy. *Blood*. 2014;124:3490-3500.
31. Hodi FS, Chesney J, Pavlick AC, et al. Combined nivolumab and ipilimumab versus ipilimumab alone in patients with advanced melanoma: 2-year overall survival outcomes in a multicentre, randomised, controlled, phase 2 trial. *Lancet Oncol*. 2016;17:1558-1568.
32. Sakuishi K, Apetoh L, Sullivan JM, Blazar BR, Kuchroo VK, Anderson AC. Targeting Tim-3 and PD-1 pathways to reverse T cell exhaustion and restore anti-tumor immunity. *J Exp Med*. 2010;207:2187-2194.
33. Gattinoni L, Klebanoff CA, Restifo NP. Paths to stemness: building the ultimate antitumour T cell. *Nat Rev Cancer*. 2012;12:671-684.
34. Baitsch L, Legat A, Barba L, et al. Extended co-expression of inhibitory receptors by human CD8 T-cells depending on differentiation, antigen-specificity and anatomical localization. *PLoS One*. 2012;7:e30852.
35. Chauvin JM, Pagliano O, Fourcade J, et al. TIGIT and PD-1 impair tumor antigen-specific CD8(+) T cells in melanoma patients. *J Clin Invest*. 2015;125:2046-2058.
36. van der Velden WJ, Herbers AH, Feuth T, Schaap NP, Donnelly JP, Blijlevens NM. Intestinal damage determines the inflammatory response and early complications in patients receiving conditioning for a stem cell transplantation. *PLoS One*. 2010;5:e15156.
37. Grogan BM, Tabellini L, Storer B, et al. Activation and expansion of CD8(+) T effector cells in patients with chronic graft-versus-host disease. *Biol Blood Marrow Transplant*. 2011;17:1121-1132.
38. Peric Z, Cahu X, Chevallier P, et al. Features of Epstein-Barr virus (EBV) reactivation after reduced intensity conditioning allogeneic hematopoietic stem cell transplantation. *Leukemia*. 2011;25:932-938.
39. Schnorfeil FM, Lichtenegger FS, Emmerig K, et al. T cells are functionally not impaired in AML: increased PD-1 expression is only seen at time of relapse and correlates with a shift towards the memory T cell compartment. *J Hematol Oncol*. 2015;8:93.
40. Kong Y, Zhang J, Claxton DF, et al. PD-1(hi)TIM-3(+) T cells associate with and predict leukemia relapse in AML patients post allogeneic stem cell transplantation. *Blood Cancer J*. 2015;5:e330.
41. Williams JB, Horton BL, Zheng Y, Duan Y, Powell JD, Gajewski TF. The EGR2 targets LAG-3 and 4-1BB describe and regulate dysfunctional antigen-specific $CD8^+$ T cells in the tumor microenvironment. *J Exp Med*. 2017;214:381-400.
42. Gros A, Robbins PF, Yao X, et al. PD-1 identifies the patient-specific CD8(+) tumor-reactive repertoire infiltrating human tumors. *J Clin Invest*. 2014;124:2246-2259.
43. Wang C, McPherson AJ, Jones RB, et al. Loss of the signaling adaptor TRAF1 causes $CD8^+$ T cell dysregulation during human and murine chronic infection. *J Exp Med*. 2012;209:77-91.
44. Buchan SL, Manzo T, Flutter B, et al. OX40- and CD27-mediated costimulation synergizes with anti-PD-L1 blockade by forcing exhausted $CD8^+$ T cells to exit quiescence. *J Immunol*. 2015;194:125-133.
45. Kovacsovics-Bankowski M, Chisholm L, Vercellini J, et al. Phase I/II clinical trial of anti-OX40, radiation and cyclophosphamide in patients with prostate cancer: immunological analysis. *J Immunother Cancer*. 2013;1(Suppl 1):P255.
46. Jensen SM, Maston LD, Gough MJ, et al. Signaling through OX40 enhances antitumor immunity. *Semin Oncol*. 2010;37:524-532.
47. Davids MS, Kim HT, Bachireddy P, et al. Ipilimumab for patients with relapse after allogeneic transplantation. *N Engl J Med*. 2016;375:143-153.
48. Bashey A, Medina B, Corringham S, et al. CTLA4 blockade with ipilimumab to treat relapse of malignancy after allogeneic hematopoietic cell transplantation. *Blood*. 2009;113:1581-1588.
49. Yared JA, Hardy N, Singh Z, et al. Major clinical response to nivolumab in relapsed/refractory Hodgkin lymphoma after allogeneic stem cell transplantation. *Bone Marrow Transplant*. 2016;51:850-852.
50. Singh AK, Porrata LF, Aljitawi O, et al. Fatal GvHD induced by PD-1 inhibitor pembrolizumab in a patient with Hodgkin's lymphoma. *Bone Marrow Transplant*. 2016;51:1268-1270.
51. Angenendt L, Schliemann C, Lutz M, et al. Nivolumab in a patient with refractory Hodgkin's lymphoma after allogeneic stem cell transplantation. *Bone Marrow Transplant*. 2016;51:443-445.
52. Albring JC, Inselmann S, Sauer T, et al. PD-1 checkpoint blockade in patients with relapsed AML after allogeneic stem cell transplantation. *Bone Marrow Transplant*. 2017;52:317-320.
53. Onizuka M, Kojima M, Matsui K, et al. Successful treatment with low-dose nivolumab in refractory Hodgkin lymphoma after allogeneic stem cell transplantation. *Int J Hematol*. 2017;106:141-145.
54. McDuffee E, Aue G, Cook L, et al. Tumor regression concomitant with steroid-refractory GvHD highlights the pitfalls of PD-1 blockade following allogeneic hematopoietic stem cell transplantation. *Bone Marrow Transplant*. 2017;52:759-761.
55. Villasboas JC, Ansell SM, Witzig TE. Targeting the PD-1 pathway in patients with relapsed classic Hodgkin lymphoma following allogeneic stem cell transplant is safe and effective. *Oncotarget*. 2016;7:13260-13264.
56. Haverkos BM, Abbott D, Hamadani M, et al. PD-1 blockade for relapsed lymphoma post-allogeneic hematopoietic cell transplant: high response rate but frequent GVHD. *Blood*. 2017;130:221-228.